Accepted to J. Chem. Phys. 10.1063/5.0114399

Symmetry-resolved CO desorption and oxidation dynamics on O/Ru(0001) probed at the C K-edge by ultrafast X-ray spectroscopy

Jerry LaRue*,[1] Boyang Liu,[2] Gabriel L. S. Rodrigues,[2] Chang Liu,[2] Jose Antonio Garrido Torres,[6] Simon Schreck,[2] Elias Diesen,[9] Matthew Weston,[2] Hirohito Ogasawara,[3] Fivos Perakis,[2] Martina Dell'Angela,[4] Flavio Capotondi,[5] Devon Ball,[1] Conner Carnahan,[1] Gary Zeri,[1] Luca Giannessi,[5] Emanuele Pedersoli,[5] Denys Naumenko,[5] Peter Amann,[10] Ivaylo Nikolov,[5] Lorenzo Raimondi,[5] Carlo Spezzani,[5] Martin Beye,[7] Johannes Voss,[6] Hsin-Yi Wang,[2] Filippo Cavalca,[2] Jörgen Gladh,[6] Sergey Koroidov,[2] Frank Abild-Pedersen,[6] Manuel Kolb,[2,6] Piter S. Miedema,[7] Roberto Costantini,[4,8] Tony F. Heinz,[6,11] Alan C. Luntz,[6] Lars G. M. Pettersson,[2] and Anders Nilsson[2]

[1]*Schmid College of Science and Technology, Chapman University, Orange, California 92866, USA*
[2]*Department of Physics, AlbaNova University Center, Stockholm University, SE-10691 Stockholm, Sweden*
[3]*SLAC National Accelerator Laboratory, 2575 Sand Hill Road, Menlo Park, California 94025, USA*
[4]*CNR-IOM, SS 14 - km 163.5, 34149 Basovizza, Trieste, Italy*
[5]*FERMI, Elettra-Sincrotrone Trieste, SS 14 - km 163.5, 34149 Basovizza, Trieste, Italy*
[6]*SUNCAT Center for Interface Science and Catalysis, SLAC National Accelerator Laboratory, 2575 Sand Hill Road, Menlo Park, California 94025, USA*
[7]*Deutsches Elektronen-Synchrotron DESY, Notkestrasse 85, 22607 Hamburg, Germany*
[8]*Physics Department, University of Trieste, Via Valerio 2, 34127 Trieste, Italy*
[9]*Fritz-Haber Institute of the Max-Planck-Society, Faradayweg 4-6, D-14195 Berlin, Germany*
[10]*Scienta Omicron AB, Danmarksgatan 22, 75323 Uppsala, Sweden*
[11]*Department of Applied Physics, Stanford University, Stanford, California 94305*
*larue@chapman.edu, (714) 744-7660

Abstract

We report on carbon monoxide desorption and oxidation induced by 400 nm femtosecond laser excitation on the O/Ru(0001) surface probed by time-resolved X-ray absorption spectroscopy (TR-XAS) at the carbon K-edge. The experiments were performed under constant background pressures of CO ($6x10^{-8}$ Torr) and O_2 ($3x10^{-8}$ Torr). Under these conditions, we detect two transient CO species with narrow 2π* peaks, suggesting little 2π* interaction with the surface. Based on polarization measurements, we find that these two species have opposing orientations: (1) CO favoring a more perpendicular orientation and (2) CO favoring a more parallel orientation with respect to the surface. We also directly detect gas-phase CO_2 using a mass spectrometer and observe weak signatures of bent adsorbed CO_2 at slightly higher X-ray energies than the 2π* region. These results are compared to previously reported TR-XAS results at the O K-edge where the CO background pressure was three times lower ($2x10^{-8}$ Torr) while maintaining the same O_2 pressure. At the lower CO pressure, in the CO 2π* region, we observed adsorbed CO and a distribution of OC–O bond lengths close to the CO oxidation transition state, with little indication of gas-like CO. The shift towards 'gas-like' CO species may be explained by the higher CO exposure, which blocks O adsorption, decreasing O coverage and increasing CO coverage. These effects decrease the CO desorption barrier through dipole-dipole interaction, while simultaneously increasing the CO oxidation barrier.

Introduction

The elementary processes that occur between molecules and metal surfaces are key to understanding heterogeneous catalytic reactions since they determine the available reaction pathways, selectivity, and kinetic rates. Insight into the details of the dynamics controlling these processes is not only important for describing catalytic reactions, but also for predicting highly efficient and selective catalysts. It is of fundamental importance to examine not only how changing the catalytic surface, but also the gas phase composition can affect these processes and, correspondingly, reaction pathways.

CO oxidation and desorption on metal surfaces have long been models for the study of reaction dynamics in catalysis.[1–8,8–22] In this study, we investigate laser-induced CO desorption and oxidation on oxygen-covered Ru(0001) under CO-rich conditions at the C K-edge using symmetry-resolved TR-XAS. We find two different CO species with different preferred orientations develop after laser excitation, each with narrow 2π* gas-like peaks, suggesting little interaction between the 2π* and the surface. At higher X-ray energies, we find weak signals for bent CO_2, showing that the CO oxidation channel is still active. We compare our results to previous results not obtained under CO-rich conditions.

Optical pump / X-ray probe studies under CO-only conditions on Ru(0001) observed a transient intermediate gas-like precursor state of CO prior to desorption.[11] This state, which had long been theorized,[23–26] traps CO in a physisorption well with little interaction with the surface and arises due to the increased rotational entropy of CO. When the experiments were repeated with oxygen-covered Ru(0001) under less CO-rich conditions than presented here, little evidence of this precursor state, or any CO gas-like states, was present.[1] Density functional theory (DFT) calculations showed that a long-range σ-driven interaction between the CO molecules and the surface due to the presence of O gives rise to a preferred perpendicular orientation of the desorbing CO. This reduces the rotational entropy of CO, and, consequently, destabilizes the associated precursor state. These results emphasize that not only is the catalytic surface a determinate of the reaction outcome, but also the gas phase composition can critically control the final reaction paths.

Experimental

We employed pump-probe spectroscopy to access the ultrafast dynamics, with the pump being a 400 nm femtosecond laser pulse and the probe a femtosecond X-ray free-electron laser (XFEL) pulse around the C K-edge. The experiments were performed using the DiProl end station at the FERMI XFEL in Trieste, Italy. FERMI is a two-stage fully seeded soft X-ray free electron laser,[27] with access to X-ray energies in the range of the carbon 2π* (~288 eV) feature. As a seeded source, FERMI provides X-ray pulses with very little time jitter with respect to the optical pump pulses. The surface science endstation (Titan) was transported from Stockholm University to FERMI and installed downstream from the permanent DiProl endstation. The endstation is equipped with standard surface-science preparation tools, including an ion-sputtering gun, sample cooling, as well as sample heating by radiation and electron bombardment. Other tools include a four-axis sample manipulator to provide both full sample translation and sample rotation; a high-efficiency and large-solid-angle fluorescence yield (FY) detector; and

beam monitors and timing tools that are used for the spatial and temporal overlapping of optical laser with the XFEL pulses.

During the pump-probe measurement, 400 nm optical laser pulses with a pulse duration of ~100 fs and laser fluence close to, but below the damage threshold for Ru(0001) induced the reaction. The subsequent temporal evolution was probed using the XFEL pulses. The optical laser and x-ray laser were collinear with respect to each other and at 3° grazing incidence with respect to the sample surface. The soft X-ray pulses were generated within the two-stage seeding scheme of the FERMI FEL[27,28] and were of ~50 fs duration. Since the XFEL laser seed and optical pump pulses are generated from the same laser system, the optical laser pump and the XFEL probe are intrinsically synchronized very closely to one another, although there is some thermal drift. This results in a time resolution of ~110 fs. A fluorescent phosphor screen was used to visualize the XFEL beam to spatially overlap the optical laser with the XFEL beam. To achieve temporal overlap, a two-step process was used. First, the tip of an in-vacuum SMA cable was moved into the overlapped beams. The XFEL and optical laser pulses both create short electronic pulses on the SMA cable that can be measured and visualized using a GHz-bandwidth oscilloscope. By adjusting the delay between optical laser and XFEL, both electronic pulses on the oscilloscope could be temporally overlapped to within a few picoseconds. In the second step, temporal overlap on the ~100 fs scale was established by monitoring the X-ray total fluorescence yield (TFY) XAS intensity from CO adsorbed on a Ru(0001) surface as a function of delay between optical laser and FEL. The ultrafast X-ray response to laser-induced CO desorption in the CO/Ru(0001) system has been well studied.[11,29] We monitored the XAS intensity at 289 eV, which is on the high-energy flank of the CO 2π* resonance.

In our measurements, a well-established surface science method[1] was initially employed to produce a clean, well-ordered Ru(0001) surface. To this end, the ruthenium crystal was treated by repeated cycles of Ne^+ sputtering and high-temperature flash annealing in an O_2 atmosphere at 1070 K. The molecular adlayer was then prepared in the following way: The sample was first dosed with 20 L (Langmuir (L) = $1x10^{-6}$ Torr for 1 s) of O_2 when the temperature dropped below 620 K. Subsequently, the sample was exposed to CO at a temperature of 170 K to reach CO saturation coverage. This procedure has been shown to give the well-known (2O+CO)/Ru(0001) honeycomb surface structure, where the O atoms sit in hollow sites in a honeycomb structure and the CO molecules sit on the top sites at the center of each hexagon.[30] During the measurements, a background gas pressure of $6x10^{-8}$ Torr CO and $3x10^{-8}$ Torr O_2 was maintained while the sample temperature remained at ~100 K. In order to have a newly prepared surface spot during the measurements the sample was continuously scanned and each spot on the sample was revisited after a cycle period of 10-20 seconds to repopulate the spots that had been previously measured. Every 2-3 hours, we cleaned the sample and prepared a fresh monolayer of CO and O using the procedure described above to ensure our sample was not contaminated.

We recorded the TR-XAS data using polarizations that were **in-plane** with respect to the Ru(0001) surface and **out-of-plane** with respect to the Ru(0001) surface at a repetition rate of 10 Hz. The central average XFEL photon energy was scanned over the desired range around the carbon K-edge resonance with a step of 0.3 eV or 0.5 eV, depending on the resonance range (e.g., pre-edge or post-edge of the 1s to 2π* resonance). The delay between the optical laser and the XFEL pulse was set to pre-defined values before recording 1,000 XFEL shots for each photon energy

and delay combination. At early timescales (-1.0 ps to 2.0 ps), data were recorded at 0.25 ps intervals. Extended time delays were recorded at 5.0 ps and 10.0 ps. We continuously measured laser-induced CO_2 desorption using a mass spectrometer to ensure that CO_2 production, and hence surface conditions, remained constant throughout the measurements (see **Supplementary Material**).

The raw experimental recorded data were post-processed based on the data analyses of the FERMI online spectrometer on a shot-to-shot basis. For this analysis, we checked the spectral intensity distribution for each XFEL shot and obtained the central photon energies, bandwidth, and intensity of each shot. In the data processing, shots with low (close to zero) intensity and large FEL bandwidth (FHWM > 0.5 eV) were filtered out. We sorted all shots based on their central photon energy into bins of 0.1 eV width. For each bin, the TFY intensity was normalized by the incident intensity and the standard error was calculated based on Poisson statistics.

Results

Figure 1 shows the C K-edge in-plane and out-of-plane TR-XAS spectra for the 2π* region of CO. Selected time slices are presented in **Figure 2**, where data are averaged over 1.0 ps time bins for better statistics. Three features are evident in the data: (1) a broad peak near 288 eV representing adsorbed CO, referred to as $CO_{(ads)}$ (2) a narrow peak centered at the CO gas phase value of 287.42 eV, referred to as $CO_{(A)}$, both in the in-plane scan; and (3) a second narrow peak between the adsorbed and gas phase energies at 287.7 eV, referred to as $CO_{(B)}$ in the out-of plane scan. After femtosecond laser excitation, the $CO_{(ads)}$ peak decreases in intensity and redshifts to lower energy. $CO_{(A)}$ and $CO_{(B)}$ peaks, without any initial intensity in the unpumped spectrum, continuously grow in strength over the 10 ps timeframe of the data. These trends can be seen in **Figure 3**, where the unpumped signal has been subtracted from the data.

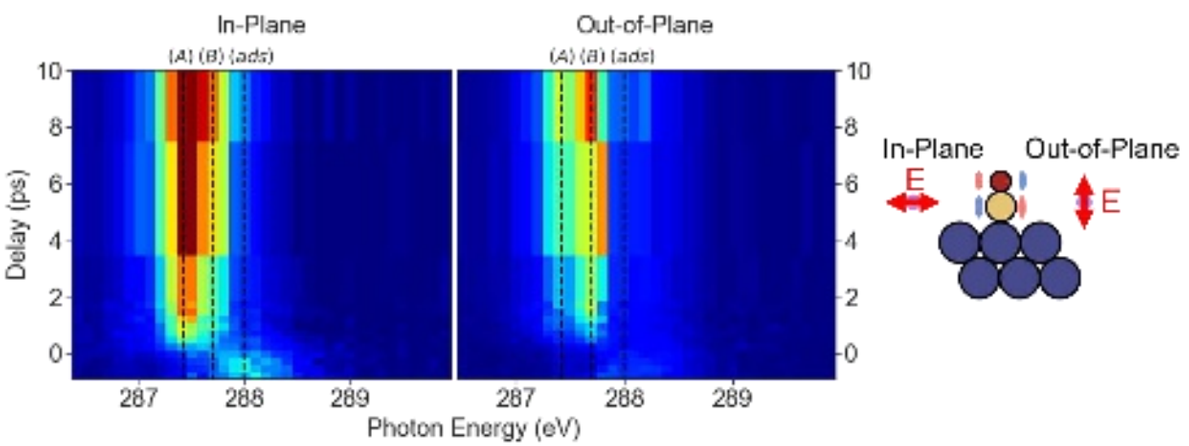

Figure 1. False color plot of the CO 2π* region TR-XAS spectra for the (**left**) in-plane and (**center**) out-of-plane polarizations. Red indicates highest intensity and blue lowest intensity. The dashed lines represent the peak positions for $CO_{(A)}$, $CO_{(B)}$, and $CO_{(ads)}$. (**Right**) The geometry of the X-ray laser polarization with respect to the surface for in-plane and out-of-plane.

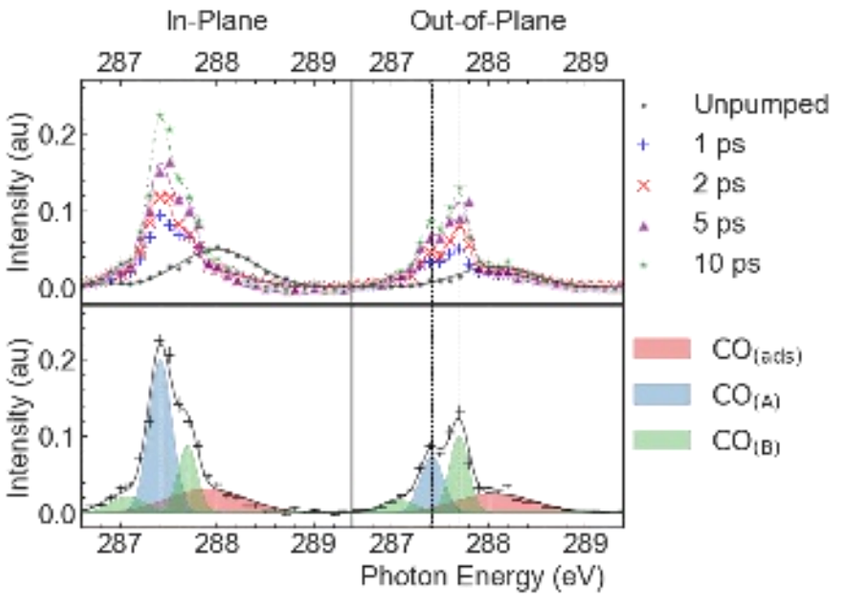

Figure 2. (**Top**) CO 2π* region TR-XAS spectra showing the (**left**) in-plane and (**right**) out-of-plane polarizations. The data is binned using 1.0 ps bins for better statistics. The dashed lines represent fits for the peaks using Gaussian profiles, as described in the text. (**Bottom**) The corresponding TR-XAS spectra fits at 10 ps time delay. The dashed vertical lines indicate the center of the fitted peaks.

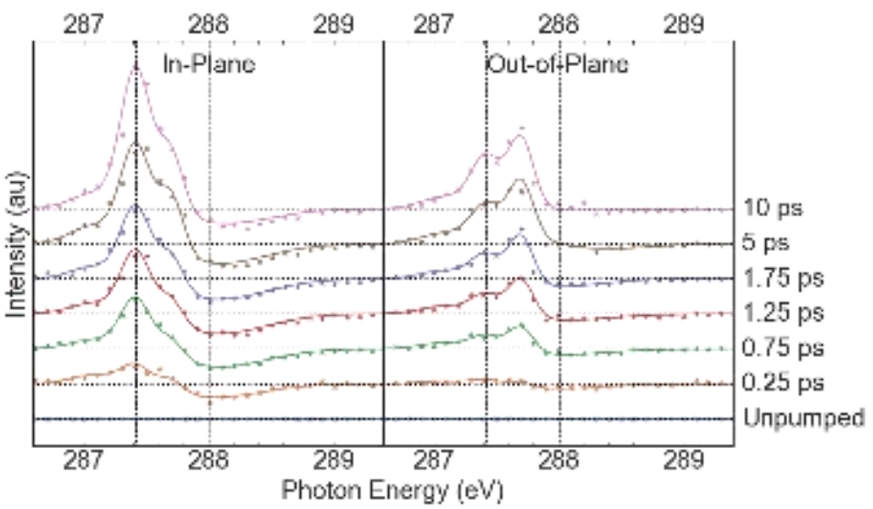

Figure 3. Changes in the CO 2π* region TR-XAS spectra relative to the unpumped system for (**left**) in-plane and (**right**) out-of-plane polarizations. The dashed vertical lines indicate the center of the fitted peaks.

We fit each of the CO peaks with a Gaussian profile. The $CO_{(ads)}$ feature is centered at 288.0 eV with a FWHM of 0.94 eV. $CO_{(A)}$ is centered at 287.42 eV[31] with a FHWM of 0.24 eV. $CO_{(B)}$ consists of two peaks, one centered at 287.7 eV with a FWHM of 0.24 eV and a broader, lower-energy peak at 287.08 eV with a FWHM 0.42 eV. See **Discussion** for more details. The top of **Figure 4** shows the transient changes of the spectral features as a function of pump-probe delay for the three CO species. The $CO_{(ads)}$ peak intensity decreases on the 0.45 ± 0.05 ps timescale, while the

intensities of the $CO_{(A)}$ and $CO_{(B)}$ peaks rapidly increase over a 0.78 ± 0.04 ps timescale, as shown by the solid lines. The $CO_{(A)}$ and $CO_{(B)}$ peaks continue to increase in intensity over the 10 ps timescale and their intensities are nearly identical to each other. The increase in intensity arises as adsorbed CO enters these gas-like states, though quantitative estimates are not possible as gas-like CO absorbs more strongly than adsorbed CO. After 2 ps, the $CO_{(ads)}$ peak starts to recover some of its original intensity but is still redshifted.

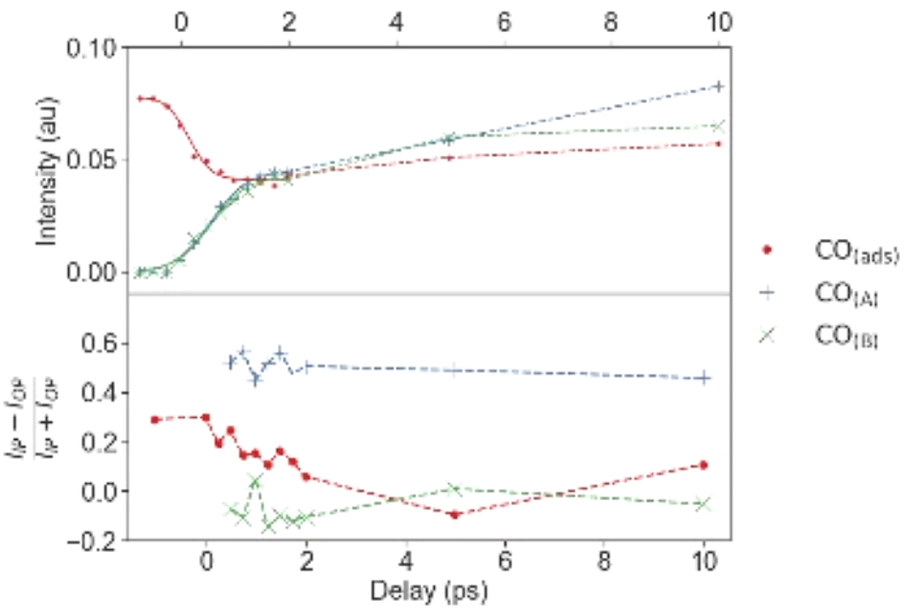

Figure 4. (**Top**) The time evolution of the TR-XAS features based on our fitting model. The in-plane and out-of-plane intensity are summed together for each CO species. Solid lines represent the evolution for each peak on the 2 ps timescale and the dashed lines are added to aid the eye. (**Bottom**) Polarization anisotropy parameter $\rho = (I_{IP} - I_{OP})/(I_{IP} + I_{OP})$ resulting from the CO fits of the spectra for different X-ray polarizations as a function of pump-probe delay. Higher values of ρ represent CO in a more perpendicular orientation (maximum value of 1) and lower values represent CO in more parallel orientation (minimum value of -1/3).

As the CO 2π* orbitals lie in the plane perpendicular to the CO molecular axis, excitation of these orbitals requires the polarization of the X-rays to be perpendicular to the CO molecular axis. For CO molecules oriented perpendicular to the surface, only in-plane absorption intensity (I_{IP}), and no out-of-plane intensity (I_{OP}), would thus be observed. For CO molecules with their axis parallel to the surface, the out-of-plane intensity would be twice that of the in-plane intensity. We calculated the relative orientations of the three different CO spectral features by calculating the polarization anisotropy parameter ρ given by the difference between the intensities of the in-plane and out-of-plane fits compared to the sum of their intensities:

$$\rho = \frac{I_{IP} - I_{OP}}{I_{IP} + I_{OP}}$$

If the CO molecule is perpendicular to the surface, ρ = 1 will result, while parallel CO will yield $\rho = -1/3$. The bottom of **Figure 4** shows the experimental value of ρ for the three different CO spectral

features as a function of delay time. After laser excitation, $CO_{(ads)}$ moves towards a more parallel orientation with respect to the surface, as indicated by the decreasing ρ value. Despite the similar peak intensities, $CO_{(A)}$ favors a more perpendicular orientation to the surface than unpumped $CO_{(ads)}$, while $CO_{(B)}$ favors a more perpendicular orientation to the surface. The orientation differences highlights that these are distinct gas-like CO species.

We confirmed that gas-phase CO_2 is produced using mass spectrometry (see **Supplementary Material**) and even see evidence that the resonant X-ray pulses enhance CO oxidation. This is likely due to the core-excited CO becoming vibrationally excited, promoting CO oxidation.[32] Despite confirmation of CO_2 formation, changes in the CO $2\pi^*$ region are dominated by CO desorption dynamics, obscuring any observable CO oxidation dynamics. Bent CO_2 has been reported as an anionic precursor to CO and O and may form in the reverse process of CO oxidation.[33–35] We recorded data at X-ray energies above the CO $2\pi^*$ resonance, up to 295 eV, where we observe bent surface CO_2 on the surface. **Figure 5** shows the TR-XAS bent CO_2 peak corresponding to a bent, weakly chemisorbed CO_2 species.[1] The integrated intensity between 293.4 eV and 294 eV is displayed on the right of **Figure 5**. Due to the σ-bond character of this state, we see more intensity in the in-plane geometry, as expected. The intensity of the signal steadily rises over the course of 10 ps, implying that this is likely driven by thermal processes of the phonon bath heating up due to electron-phonon coupling.

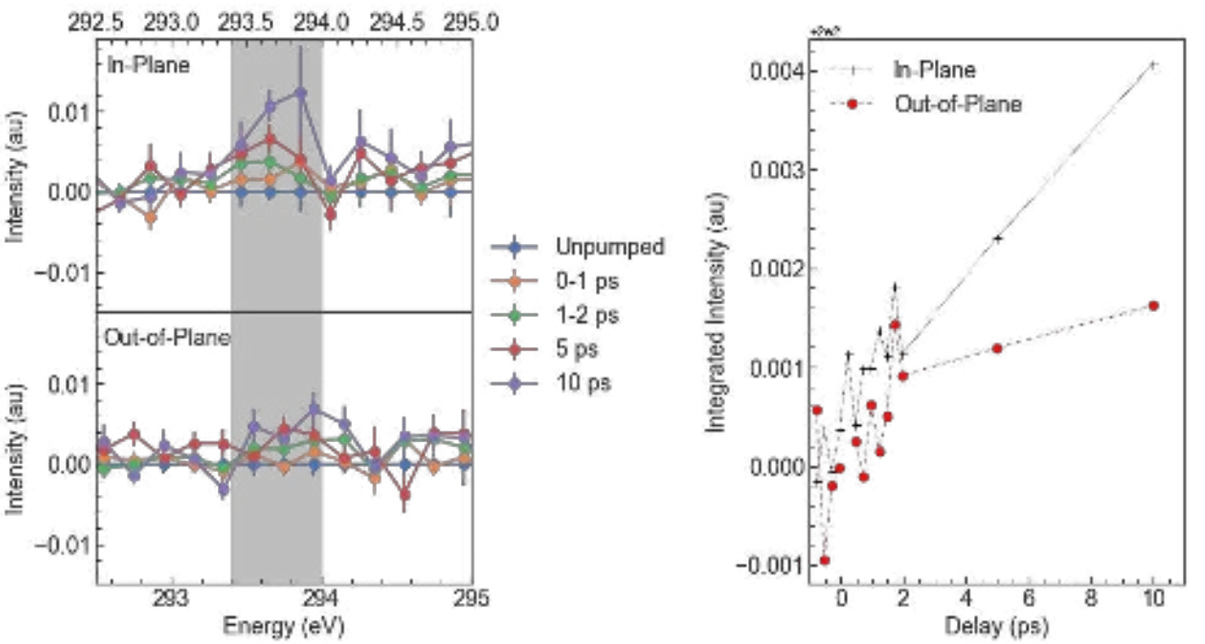

Figure 5. (**Left**) Difference spectra of the bent CO_2 region grouped with 1.0 ps time bins and 0.2 eV energy bins for better statistics. The unpumped data are subtracted from all time bins. (**Right**) The change in integrated intensities from 293.4 eV to 294.0 eV using 0.25 ps time steps.

Discussion

In our measurements, we initially prepared the CO+O honeycomb structure, however, our experimental conditions required continuous background pressures of CO and O_2 at ~100 K.

Below 149 K, O forms a 2x1 structure and CO forms a disordered overlayer with a coverage of 0.36 ML.[22] Some of the O that adsorbs to replace previously reacted O may adsorb in the p(2x1) phase. O_2 requires two nearby vacancies to dissociatively adsorb on the surface. Isolated O vacancies would likely remain as vacancies until a nearby vacancy develops to allow O_2 to dissociate as the diffusion barrier for O on Ru(0001) is relatively high, between 0.55 eV and 0.70 eV.[36] Adsorbed CO is known to block the adsorption of other species, including O_2, further increasing O vacancies. As a result, our surface likely has a lower O coverage and higher CO coverage than the initially prepared CO+O honeycomb structure. Mass spectrometry data shows that CO_2 desorption yields do not change over time, indicating that the surface has reached a steady state. See **Supplementary Material**.

Using the polarization dependence of the integrated intensities of the unpumped spectra, we calculate an average tilt angle of initial state of the adsorbed CO to be 42° ± 3° from the surface normal. See **Supplementary Material** for details on the calculation. Previous studies have reported CO tilt angles on O/Ru(0001). On the p(2x2)(O+CO)/Ru(0001) surface (0.25 ML O), CO tilt angles of 12.6 ± 4.6 ° were inferred from LEED data at 120 K, while, on the p(2x2)(2O+CO)/Ru(0001) surface (0.50 ML O in honeycomb structure), no information on tilt angles were reported.[30,37] The tilt angle of CO towards neighboring O atoms has been calculated to be up to 41° on the (2x2)(2CO+O)/Ru(0001) surface with less than a 0.03 eV barrier from the perpendicular position .[38] The coverage and structure of O on the surface impact the CO tilt angles, and the resulting overlayer structure from the experimental conditions seems to favor larger CO tilt angles than similar previous studies.

On the sub-picosecond timescale after laser excitation, the $CO_{(ads)}$ 2π* intensity redshifts and decreases in strength. Previous investigations of the dynamics induced by ultrafast laser pulses for CO+ O on Ru(0001) have found that electron- and phonon-mediated processes both play a central role in CO oxidation and desorption.[2,12] In laser-induced chemical reactivity on Ru(0001), the frustrated rotation of CO, the CO internal stretch, and the O-Ru surface vibration[39,40] are excited on the sub-picosecond timescale by coupling to the electron bath.[41,42] Excitation of the frustrated rotation of CO can lead to a small redshift in the 2π* peak, and excitation of the internal stretch can cause a modest decrease in the XAS intensity.[42] Prior studies of CO on Ni(100) have shown that there is a redshift and broadening of the CO 2π* peak as CO shifts from top-site to hollow-site.[43] The broadening of the adsorbed peak is due to stronger interaction with the surface. Due to the emergence of other features overlapping with the adsorbed CO intensity, it is difficult to identify whether the CO 2π* peak broadens, though prior studies of CO on Ru(0001) and O/Ru(0001) have reported that CO does become more highly coordinated immediately after laser excitation.[1,11]

The intensities of the $CO_{(A)}$ and $CO_{(B)}$ peaks continuously increases over the 10 ps timeframe that the data were recorded. These gradual increases in intensity suggest that hot phonon modes, which heat up on the picosecond timescale due to electron-phonon coupling, are required for CO desorption, consistent with prior studies.[11,44,45] The narrowness of both peaks (FWHM of 0.24 eV) suggests that there is a strong reduction in the interaction of the CO 2π* system with the surface, similar to the previously reported precursor state.[11,22] This transient precursor state was experimentally observed on CO/Ru(0001) in pump-probe experiments by exciting with 400-nm femtosecond laser pulses and recording the time-resolved X-ray absorption spectroscopy (TR-

XAS) signal for the O K-edge using an X-ray free electron laser (XFEL).[11] Subsequent pump-probe studies at the O K-edge found little evidence of this precursor state when O was coadsorbed on the Ru(0001) surface. The free energy surfaces for CO desorbing from CO/Ru(0001) and 2O-CO/Ru(0001) have been previously calculated using DFT.[44,46–49] On Ru(0001), the 5σ state of CO exhibits a repulsive interaction with the surface due to Pauli repulsion,[44] while the CO π system facilitates bonding with the surface. The DFT results showed that when present, the O atoms pull electron density away from neighboring Ru atoms, reducing the σ-repulsion between CO and the metal surface,[44] giving rise to the long-range interaction. Since the 5σ lies along the intermolecular axis, this CO-surface interaction only occurs in the perpendicular orientation, leading to a preferred perpendicular orientation of the desorbing CO. At such long distances, it is highly unlikely that the 2π* system would be interacting with the surface, and we would expect to see CO gas-like behavior in the spectra. The gas-like behavior and favored perpendicular orientation to the surface are consistent with the behavior of $CO_{(A)}$, though it is unclear whether the $CO_{(A)}$ molecules are trapped in a physisorption state.

TD-DFT calculations were performed to simulate the polarization independent CO 2π* C K-edge X-ray spectra as CO desorbs from the O/Ru(0001) surface in the parallel and perpendicular orientations (See **Supplementary Material**). We examined three different oxygen coverages, motivated by the possibility that we have less surface oxygen than the prepared (2O+CO)/Ru(0001) honeycomb structure. The first is the honeycomb structure that arises from the saturated coadsorption of CO and O. In this structure, O has a 0.5 monolayer (ML) coverage, where 1 ML is defined as the ratio of the number of adsorbates to the number of surface metal atoms. Two modified structures were added to represent half the oxygen coverage of the honeycomb structure (0.25 ML), as illustrated in **Figure 6**. Both modified structures gave rise to indistinguishable X-ray spectra. For perpendicular CO, the 2π* forms an antibonding orbital with the metal d_π states, which increases the 2π* energy. When the CO tilts from the perpendicular position to parallel, the symmetry of the $2\pi_x^*$ and $2\pi_y^*$ is broken, as one orbital is pointed toward the surface and the other is parallel to it. In the parallel orientation, there is an increased interaction between the 2π* and the surface, making possible bonding contributions with the metal and lowering the 2π* energy. These bonding contributions appear in the spectra below 287 eV for $CO_{(B)}$, while the main peak intensity is at 287.7 eV. There is a much smaller chemical shift from the gas phase to the interacting state for parallel CO compared to perpendicular CO. As the surface-CO distance increases, there is a significant lowering of the main peak intensity for parallel CO compared to perpendicular CO, where we almost have gas phase CO 2π* character at 2.3 Å. For parallel CO, the bonding interaction is almost absent by 4.0 Å, although still weakly observed. At 7.0 Å, as expected, the surface interactions disappear for both orientations, and the CO is in the gas phase.

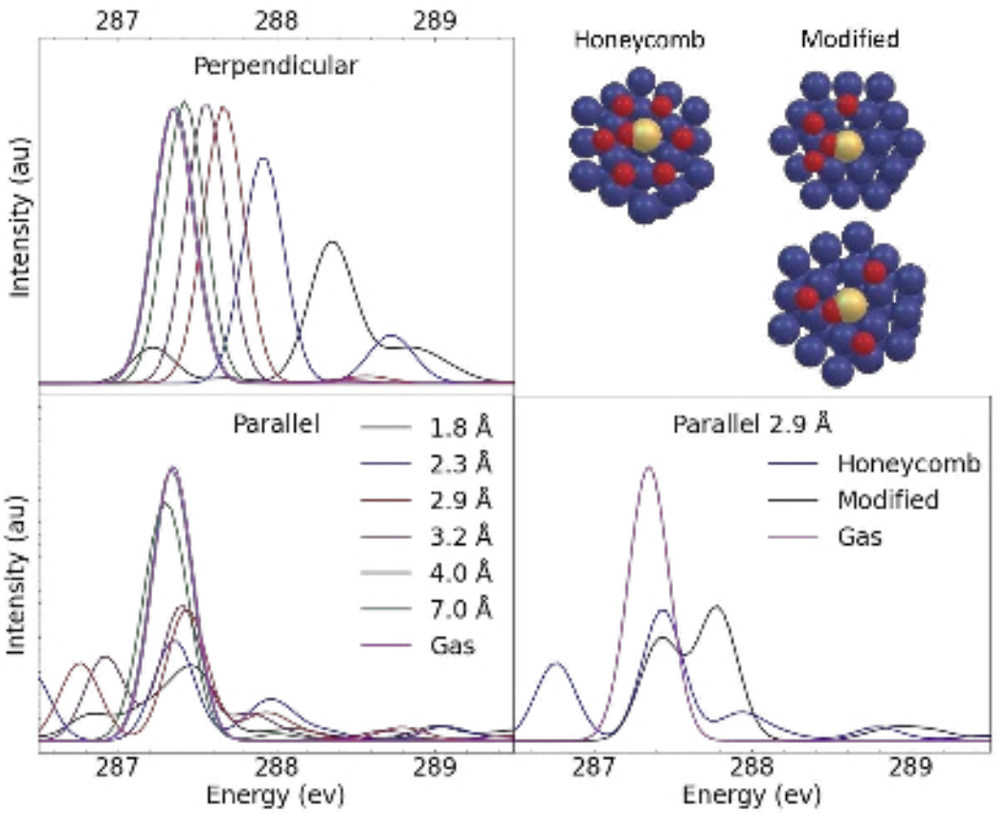

Figure 6. Calculated XAS spectra at the C K-edge. A range of CO-surface distances for (**top left**) perpendicular CO and (**bottom left**) parallel CO on O/Ru(0001) in the honeycomb structure. (**Top right**) The honeycomb structure of O/Ru(0001), as well as two modified structures with half the O coverage of the honeycomb structure. (**Bottom right**) CO at 2.9 Å above the O/Ru(0001) honeycomb structure and the two modified O adlayers. Only one of the modified spectra is shown as the two structures yielded indistinguishable spectra.

We have previously reported TR-XAS CO oxidation at the O K-edge under similar conditions where the pressure of CO was three times lower than reported here ($2x10^{-8}$ Torr), while maintaining the same O_2 pressure.[1,29,44] It is important to note that these experiments were not polarization sensitive. We refer to these prior studies as the "low CO exposure" data and the current study as the "high CO exposure" data.

For the previously reported low CO exposure, virtually no gas-like CO was detected,[1] although some gas-like CO may have been present as a small shoulder of the main CO peak between 534 eV and 536 eV. If present, this would indicate a low concentration of gas-like CO. The $2\pi^*$ region was dominated by states along the CO oxidation pathway. In stark contrast, the results presented here show almost exclusively CO desorption dynamics in the $2\pi^*$ region, with little evidence of CO oxidation. It appears that the high CO exposure strongly favors CO desorption over oxidation, in contrast with low CO exposure.

In a recent paper by Tetenoire *et al.*,[50] the energy barriers associated with CO oxidation and desorption on the O/Ru(0001) surface were calculated as a function of CO coverage. The authors

studied CO coverages of 0.25 ML (low), 0.375 ML (intermediate), and 0.50 ML (high) on the p(2x1) O structure (0.5 ML O), as well as the honeycomb structure, which has a CO coverage of 0.25 ML. They find that the desorption barrier drops significantly with CO coverage: by 1.0 eV from the low and honeycomb CO coverages to the intermediate CO coverage, and by another 0.1 eV from the intermediate to high CO coverage. This decrease arises from the CO-CO dipole interaction that competes against CO binding to the surface. With the high CO exposure, the surface CO would more quickly block O adsorption sites, increasing the concentration of CO on the surface and pushing the system towards the high CO coverage behavior predicted by Tetenoire *et al*.

Tetenoire *et al*. also predict the existence of a physisorption well for CO desorption at intermediate and high coverages. The minimum of the CO-surface physisorption potential well varies with CO adsorption site and surface coverage but is generally 1 – 5 Å above the equilibrium CO-surface bond distance. One of the most favorable physisorption wells arises from the intermediate coverage with CO desorbing from a location between a top site and fcc site, with a tilt towards the fcc site. At these CO-surface distances, our calculated XAS spectra show that the 2π* peak for the perpendicular CO has gas-like behavior.

Between 2.8 Å and 3.3 Å, the calculated XAS spectra for parallel CO with O in the honeycomb structure shows the higher energy 2π* antibonding state remains constant at an energy higher than the gas phase CO peak. For the structures with half the O coverage, the calculated shift is even higher in energy. The experimental shift is between the two indicating that we likely have an O coverage between 0.25 ML and 0.5 ML. The lower energy 2π* bonding peak has a strong dependence on CO-surface distance between 2.3 Å and 3.3 Å. A collection of molecules in this range would give rise to XAS spectra that feature a narrow higher-energy antibonding peak and a broader, lower-intensity, lower-energy bonding peak, corresponding to our observations. This suggests that the more parallel $CO_{(A)}$ is trapped within these CO-surface bond distances.

Under low CO exposure, little gas-like CO was observed. On the other hand, experiments probing gas-like products have shown that the primary species leaving the surface in laser-induced chemistry on CO/O/Ru(0001) is CO, not CO_2.[2] The origin of the lack of signatures of gas-like CO in the low CO exposure TR-XAS data remains unclear. It may be that the existence of a physisorbed (precursor) state, where CO concentration can build up, is a requirement for strong detection of gas-like CO in TR-XAS, similar to that found in CO desorption on Ru(0001).[11] The likely different surface coverages of CO and O also play a key role in the balance between CO desorption and CO oxidation.

Tetenoire *et al*. show that the CO oxidation transition-state barrier initially decreases from low CO coverage to intermediate CO coverage by 0.4 eV, but then sharply increases by 1.2 eV at high CO coverage. The CO oxidation transition state barrier for both the low and intermediate CO coverages is lower than for the honeycomb structure, which is still 0.34 eV lower than the high coverage limit. In the low CO exposure experiments, O was readsorbing on the surface just above 100 K,[1] well below the honeycomb transition temperature of around 214 K.[22] The low CO exposure experiments may be closer to the intermediate CO coverage with an O structure of p(2x1) than to the honeycomb structure. At higher X-ray energies, between 293 eV and 294 eV, we directly observe the adsorbed bent CO_2 state. The intensity of this feature steadily increases over 10 ps. It is likely that the CO oxidation signature is present in the 2π* region but is simply drowned out by the large CO gas-like features. As CO desorbs from the surface immediately after laser

excitation, the system would transition from the high coverage limit to intermediate or low coverages, bringing down the activation barrier for CO oxidation. In other words, some CO may need to desorb prior to the CO oxidation channel becoming favorable.

Conclusion

We recorded TR-XAS spectra showing the time evolution of CO desorption and CO oxidation on O/Ru(0001). The 1s - $2\pi^*$ resonance of adsorbed CO rapidly undergoes a redshift and decrease in intensity after laser excitation, potentially from the excitation of the frustrated rotation, internal stretch, and/or moving to more highly-coordinated sites. At longer timescales, some CO molecules detach from the surface with a reduced π^* interaction with the surface. Two states are observed having differing orientations. These results are in stark contrast with similar experiments performed previously under lower CO exposure conditions, where no physisorbed or gas-like CO was observed. We expect the higher CO exposure of this study to lead to a higher CO coverage and lower O coverage, decreasing the barriers for CO desorption and potentially increasing the barriers for CO oxidation. While the dominant pathway is CO desorption, we do still observe a relatively weak feature at high X-ray energies associated with bent CO_2.

Supplemental Material

See Supplemental Material for mass spectrometer data, calculation of CO tilt angles, and details of XAS spectra calculations.

Acknowledgements

Research by the SLAC participants was supported by U.S. Department of Energy, Office of Science, Office of Basic Energy Sciences, Chemical Sciences, Geosciences, and Biosciences Division, Catalysis Science Program to the Ultrafast Catalysis FWP 100435 at SLAC National Accelerator Laboratory under Contract No. DE-AC02- 76SF00515. Research based in Sweden was supported by the Knut and Alice Wallenberg Foundation under Grant No 2016.0042 and the Swedish Research Council under Grant No 2013-8823, The research used resources of the National Energy Research Scientific Computing Center, a DOE Office of Science User Facility supported by the Office of Science of the U.S. Department of Energy under Contract No. DE-AC02-05CH11231. The authors acknowledge the continuous support of the FERMI team during the setting up and operation of the XFEL source for the experiment. M.B and P.S.M acknowledge funding from the Helmholtz association (VH-NG-1005). M.D.A and R.C. acknowledge support from the SIR grant SUNDYN [Nr RBSI14G7TL, CUP B82I15000910001] of the Italian MIUR. Part of the calculations were performed using resources provided by the Swedish National Infrastructure for Computing (SNIC) at the HPC2N and NSC centers.

Conflicts of interest

The authors have no conflicts of interest to disclose.

Data Availability Statement

The data that support the findings of this study are available from the corresponding author upon reasonable request.

References

(1) Öström, H.; Öberg, H.; Xin, H.; LaRue, J.; Beye, M.; Dell'Angela, M.; Gladh, J.; Ng, M. L.; Sellberg, J. A.; Kaya, S.; Mercurio, G.; Nordlund, D.; Hantschmann, M.; Hieke, F.; Kühn, D.; Schlotter, W. F.; Dakovski, G. L.; Turner, J.; Minitti, M. P.; Mitra, A.; Moeller, S. P.; Föhlisch, A.; Wolf, M., F.; Wurth, W.; Persson, M.; Nørskov, J. K.; Abild-Pedersen, F.; Ogasawara, H.; Pettersson, L. G. M.; Nilsson, A. Probing the Transition State Region in Catalytic CO Oxidation on Ru. *Science* **2015**, *347* (6225), 978–983. https://doi.org/10.1126/science.1261747.

(2) Bonn, M.; Funk, S.; Hess, C.; Denzler, D. N.; Stampfl, C.; Scheffler, M.; Wolf, M.; Ertl, G. Phonon- versus Electron-Mediated Desorption and Oxidation of CO on Ru(0001). *Science* **1999**, *285* (5430), 1042–1045. https://doi.org/DOI 10.1126/science.285.5430.1042.

(3) Böttcher, A.; Niehus, H.; Schwegmann, S.; Over, H.; Ertl, G. CO Oxidation Reaction over Oxygen-Rich Ru(0001) Surfaces. *J. Phys. Chem. B* **1997**, *101* (51), 11185–11191. https://doi.org/10.1021/jp9726899.

(4) Gao, F.; Goodman, D. W. CO Oxidation over Ruthenium: Identification of the Catalytically Active Phases at near-Atmospheric Pressures. *Phys. Chem. Chem. Phys.* **2012**, *14* (19), 6688. https://doi.org/10.1039/c2cp40121e.

(5) Grabow, L. C.; Hvolbaek, B.; Nørskov, J. K. Understanding Trends in Catalytic Activity: The Effect of Adsorbate-Adsorbate Interactions for CO Oxidation over Transition Metals. *Top. Catal.* **2010**, *53* (5–6), 298–310. https://doi.org/10.1007/s11244-010-9455-2.

(6) LaRue, J. L.; Katayama, T.; Lindenberg, A.; Fisher, A. S.; Öström, H.; Nilsson, A.; Ogasawara, H. THz-Pulse-Induced Selective Catalytic CO Oxidation on Ru. *Phys. Rev. Lett.* **2015**, *115* (3), 036103. https://doi.org/10.1103/PhysRevLett.115.036103.

(7) Madey, T. E.; Albert Engelhardt, H.; Menzel, D. Adsorption of Oxygen and Oxidation of CO on the Ruthenium (001) Surface. *Surf. Sci.* **1975**, *48* (2), 304–328. https://doi.org/10.1016/0039-6028(75)90409-4.

(8) Peden, F.; Goodman, D. W. Kinetics of CO Oxidation over Ru(0001). *J. Phys. Chem.* **1986**, *90* (178), 1360–1365.

(9) Over, H.; Muhler, M. Catalytic CO Oxidation over Ruthenium - Bridging the Pressure Gap. *Prog. Surf. Sci.* **2003**, *72* (1–4), 3–17. https://doi.org/10.1016/S0079-6816(03)00011-X.

(10) Haruta, M.; Kobayashi, T.; Sano, H.; Yamada, N. Novel Gold Catalysts for the Oxidation of Carbon Monoxide at a Temperature Far Below 0 °C. *Chem. Lett.* **1987**, *16* (2), 405–408. https://doi.org/10.1246/cl.1987.405.

(11) Dell'Angela, M.; Anniyev, T.; Beye, M.; Coffee, R.; Föhlisch, a; Gladh, J.; Katayama, T.; Kaya, S.; Krupin, O.; LaRue, J.; Møgelhøj, a; Nordlund, D.; Nørskov, J. K.; Öberg, H.; Ogasawara, H.; Öström, H.; Pettersson, L. G. M.; Schlotter, W. F.; Sellberg, J. A.; Sorgenfrei, F.; Turner, J. J.; Wolf, M.; Wurth, W.; Nilsson, A. Real-Time Observation of Surface Bond Breaking with an x-Ray Laser. *Science* **2013**, *339* (6125), 1302–1305. https://doi.org/10.1126/science.1231711.

(12) Gladh, J.; Hansson, T.; Öström, H. Electron- and Phonon-Coupling in Femtosecond Laser-Induced Desorption of CO from Ru(0001). *Surf. Sci.* **2013**, *615*, 65–71. https://doi.org/10.1016/j.susc.2013.05.002.

(13) Böttcher, A.; Conrad, H.; Niehus, H. Characterization of Oxygen Phases Created during Oxidation of Ru(0001). *J. Chem. Phys.* **2000**, *112* (10), 4779–4787. https://doi.org/10.1063/1.481034.

(14) Miller, D.; Sanchez Casalongue, H.; Bluhm, H.; Ogasawara, H.; Nilsson, A.; Kaya, S. Different Reactivity of the Various Platinum Oxides and Chemisorbed Oxygen in CO Oxidation on Pt(111). *J. Am. Chem. Soc.* **2014**, *136* (17), 6340–6347. https://doi.org/10.1021/ja413125q.

(15) Bashlakov, D. L.; Juurlink, L. B. F.; Koper, M. T. M.; Yanson, A. I. Subsurface Oxygen on Pt(111) and Its Reactivity for CO Oxidation. *Catal. Lett.* **2012**, *142* (1), 1–6. https://doi.org/10.1007/s10562-011-0730-z.

(16) Öberg, H.; Gladh, J.; Marks, K.; Ogasawara, H.; Nilsson, a.; Pettersson, L. G. M.; Öström, H. Indication of Non-Thermal Contribution to Visible Femtosecond Laser-Induced CO Oxidation on Ru(0001). *J. Chem. Phys.* **2015**, *143* (7), 74701. https://doi.org/doi:http://dx.doi.org/10.1063/1.4928646.

(17) Öberg, H.; Gladh, J.; Dell'Angela, M.; Anniyev, T.; Beye, M.; Coffee, R.; Föhlisch, A.; Katayama, T.; Kaya, S.; Larue, J.; Møgelhøj, A.; Nordlund, D.; Ogasawara, H.; Schlotter, W. F.; Sellberg, J. A.; Sorgenfrei, F.; Turner, J.; Wolf, M.; Wurth, W.; Öström, H.; Nilsson, A.; Nørskov, J. K. K.; Pettersson, L. G. M. Optical Laser-Induced CO Desorption from Ru(0001) Monitored with a Free-Electron X-Ray Laser: DFT Prediction and X-Ray Confirmation of a Precursor State. *Surf. Sci.* **2015**, *640*, 80–88. https://doi.org/10.1016/j.susc.2015.03.011.

(18) Lee, H. I.; White, J. M. Carbon-Monoxide Oxidation Over Ru (001). *J. Catal.* **1980**, *63* (1), 261–264. https://doi.org/10.1016/0021-9517(80)90078-0.

(19) Berlowitz, P. J.; Peden, C. H. F.; Goodman, D. W. Kinetics of CO Oxidation on Single-Crystal Pd, Pt, and Ir. *J. Phys. Chem.* **1988**, *92* (18), 5213–5221. https://doi.org/10.1021/j100329a030.

(20) Wheeler, M. C.; Reeves, C. T.; Seets, D. C.; Mullins, C. B. Experimental Study of CO Oxidation by an Atomic Oxygen Beam on Pt(111), Ir(111), and Ru(001). *J. Chem. Phys.* **1998**, *108* (7), 3057. https://doi.org/10.1063/1.475693.

(21) Goodman, D. W.; Peden, C. H. F.; Chen, M. S. CO Oxidation on Ruthenium: The Nature of the Active Catalytic Surface. *Surf. Sci.* **2007**, *601* (23), 18–20. https://doi.org/10.1016/j.susc.2007.09.042.

(22) Gladh, J.; Öberg, H.; Pettersson, L. G. M. G. M. M.; Öström, H. Detection of Adsorbate Overlayer Structural Transitions Using Sum-Frequency Generation Spectroscopy. *Surf. Sci.* **2015**, *633*, 77–81. https://doi.org/10.1016/j.susc.2014.11.006.

(23) Cassuto, A.; King, D. A. Rate Expressions for Adsorption and Desorption-Kinetics with Precursor States and Lateral Interactions. *Surf. Sci.* **1981**, *102* (2–3), 388–404. https://doi.org/10.1016/0039-6028(81)90036-4.

(24) Doren, D. J.; Tully, J. C. Precursor-Mediated Adsorption and Desorption - A Theoretical-Analysis. *Langmuir* **1988**, *4* (2), 256–268. https://doi.org/10.1021/la00080a004.

(25) Kisliuk, P. The Sticking Probabilities of Gases Chemisorbed on the Surfaces of Solids. *J. Phys. Chem. Solids* **1957**, *3* (1–2), 95–101. https://doi.org/10.1016/0022-3697(57)90054-9.

(26) Doren, D. J.; Tully, J. C. Dynamics of Precursor-Mediated Chemisorption. *J. Chem. Phys.* **1991**, *94* (12), 8428–8440. https://doi.org/10.1063/1.460076.

(27) Allaria, E.; Castronovo, D.; Cinquegrana, P.; Craievich, P.; Dal Forno, M.; Danailov, M. B.; D'Auria, G.; Demidovich, A.; De Ninno, G.; Di Mitri, S.; Diviacco, B.; Fawley, W. M.; Ferianis, M.; Ferrari, E.; Froehlich, L.; Gaio, G.; Gauthier, D.; Giannessi, L.; Ivanov, R.; Mahieu, B.; Mahne, N.; Nikolov, I.; Parmigiani, F.; Penco, G.; Raimondi, L.; Scafuri, C.; Serpico, C.; Sigalotti, P.; Spampinati, S.; Spezzani, C.; Svandrlik, M.; Svetina, C.; Trovo, M.; Veronese, M.; Zangrando, D.; Zangrando, M. Two-Stage

Seeded Soft-X-Ray Free-Electron Laser. *Nat. Photonics* **2013**, *7* (11), 913–918. https://doi.org/10.1038/nphoton.2013.277.

(28) Allaria, E.; Appio, R.; Badano, L.; Barletta, W. A.; Bassanese, S.; Biedron, S. G.; Borga, A.; Busetto, E.; Castronovo, D.; Cinquegrana, P.; Cleva, S.; Cocco, D.; Cornacchia, M.; Craievich, P.; Cudin, I.; D'Auria, G.; Dal Forno, M.; Danailov, M. B.; De Monte, R.; De Ninno, G.; Delgiusto, P.; Demidovich, A.; Di Mitri, S.; Diviacco, B.; Fabris, A.; Fabris, R.; Fawley, W.; Ferianis, M.; Ferrari, E.; Ferry, S.; Froehlich, L.; Furlan, P.; Gaio, G.; Gelmetti, F.; Giannessi, L.; Giannini, M.; Gobessi, R.; Ivanov, R.; Karantzoulis, E.; Lonza, M.; Lutman, A.; Mahieu, B.; Milloch, M.; Milton, S. V.; Musardo, M.; Nikolov, I.; Noe, S.; Parmigiani, F.; Penco, G.; Petronio, M.; Pivetta, L.; Predonzani, M.; Rossi, F.; Rumiz, L.; Salom, A.; Scafuri, C.; Serpico, C.; Sigalotti, P.; Spampinati, S.; Spezzani, C.; Svandrlik, M.; Svetina, C.; Tazzari, S.; Trovo, M.; Umer, R.; Vascotto, A.; Veronese, M.; Visintini, R.; Zaccaria, M.; Zangrando, D.; Zangrando, M. Highly Coherent and Stable Pulses from the FERMI Seeded Free-Electron Laser in the Extreme Ultraviolet. *Nat. Photonics* **2012**, *6* (10), 699–704. https://doi.org/10.1038/nphoton.2012.233.

(29) Nilsson, A.; LaRue, J.; Öberg, H.; Ogasawara, H.; Dell'Angela, M.; Beye, M.; Öström, H.; Gladh, J.; Nørskov, J. K. K.; Wurth, W.; Abild-Pedersen, F.; Pettersson, L. G. M. Catalysis in Real Time Using X-Ray Lasers. *Chem. Phys. Lett.* **2017**, *675*. https://doi.org/10.1016/j.cplett.2017.02.018.

(30) Narloch, B.; Held, G.; Menzel, D. Structural Rearrangement by Coadsorption - a LEED-IV Determination of the Ru(001)-p(2x2)(2O+CO) Structure. *Surf. Sci.* **1994**, *317* (1–2), 131–142. https://doi.org/10.1016/0039-6028(94)90260-7.

(31) Föhlisch, A.; Hasselström, J.; Karis, O.; Menzel, D.; Mårtensson, N.; Nilsson, A. Vibrational Fine Structure in Core Level Photoelectron Lines of Adsorbed Molecules: System Dependent Effects. *J. Electron Spectrosc. Relat. Phenom.* **1999**, *101–103*, 303–308. https://doi.org/10.1016/S0368-2048(98)00499-X.

(32) Schreck, S.; Diesen, E.; LaRue, J.; Ogasawara, H.; Marks, K.; Nordlund, D.; Weston, M.; Beye, M.; Cavalca, F.; Perakis, F.; Sellberg, J.; Eilert, A.; Kim, K. H.; Coslovich, G.; Coffee, R.; Krzywinski, J.; Reid, A.; Moeller, S.; Lutman, A.; Öström, H.; Pettersson, L. G. M.; Nilsson, A. Atom-Specific Activation in CO Oxidation. *J. Chem. Phys.* **2018**, *149* (23), 234707. https://doi.org/10.1063/1.5044579.

(33) Freund, H.-J.; Roberts, M. W. Surface Chemistry of Carbon Dioxide. *Surf. Sci. Rep.* **1996**, *25* (8), 225–273. https://doi.org/10.1016/S0167-5729(96)00007-6.

(34) Taifan, W.; Boily, J.-F.; Baltrusaitis, J. Surface Chemistry of Carbon Dioxide Revisited. *Surf. Sci. Rep.* **2016**, *71* (4), 595–671. https://doi.org/10.1016/j.surfrep.2016.09.001.

(35) Burghaus, U. Surface Chemistry of CO2 – Adsorption of Carbon Dioxide on Clean Surfaces at Ultrahigh Vacuum. *Prog. Surf. Sci.* **2014**, *89* (2), 161–217. https://doi.org/10.1016/j.progsurf.2014.03.002.

(36) Renisch, S.; Schuster, R.; Wintterlin, J.; Ertl, G. Dynamics of Adatom Motion under the Influence of Mutual Interactions: O/Ru(0001). *Phys. Rev. Lett.* **1999**, *82* (19), 3839–3842. https://doi.org/10.1103/PhysRevLett.82.3839.

(37) Narloch, B.; Menzel, G. H. D. A LEED-IV Determination of the Ru (001)-p (2X2)(O+CO) Structure : A Coadsorbate-Induced Molecular Tilt. *Surf. Sci.* **1995**, *6028* (001).

(38) Stampfl, C.; Scheffler, M. Energy Barriers and Chemical Properties in the Coadsorption of Carbon Monoxide and Oxygen on Ru(0001). *Phys. Rev. B* **2002**, *65* (15), 1–11. https://doi.org/10.1103/PhysRevB.65.155417.

(39) Bonn, M.; Hess, C.; Funk, S.; Miners, J. H.; Persson, B. N. J.; Wolf, M.; Ertl, G. Femtosecond Surface Vibrational Spectroscopy of CO Adsorbed on Ru(001) during Desorption. *Phys. Rev. Lett.* **2000**, *84* (20), 4653–4656. https://doi.org/10.1103/PhysRevLett.84.4653.

(40) Fournier, F.; Zheng, W.; Carrez, S.; Dubost, H.; Bourguignon, B. Vibrational Dynamics of Adsorbed Molecules under Conditions of Photodesorption: Pump-Probe SFG Spectra of CO/Pt(111). *J. Chem. Phys.* **2004**, *121* (10), 4839–4847. https://doi.org/10.1063/1.1778138.

(41) Beye, M.; Öberg, H.; Xin, H.; Dakovski, G. L.; Dell'Angela, M.; Föhlisch, A.; Gladh, J.; Hantschmann, M.; Hieke, F.; Kaya, S.; Kühn, D.; LaRue, J.; Mercurio, G.; Minitti, M. P.; Mitra, A.; Moeller, S. P.; Ng, M. L.; Nilsson, A.; Nordlund, D.; Nørskov, J.; Öström, H.; Ogasawara, H.; Persson, M.; Schlotter, W. F.; Sellberg, J. A.; Wolf, M.; Abild-Pedersen, F.; Pettersson, Lars. G. M.; Wurth, W. Chemical Bond Activation Observed with an X-Ray Laser. *J. Phys. Chem. Lett.* **2016**, *7* (18), 3647–3651. https://doi.org/10.1021/acs.jpclett.6b01543.

(42) Diesen, E.; Wang, H.-Y.; Schreck, S.; Weston, M.; Ogasawara, H.; LaRue, J.; Perakis, F.; Dell'Angela, M.; Capotondi, F.; Giannessi, L.; Pedersoli, E.; Naumenko, D.; Nikolov, I.; Raimondi, L.; Spezzani, C.; Beye, M.; Cavalca, F.; Liu, B.; Gladh, J.; Koroidov, S.; Miedema, P. S.; Costantini, R.; Heinz, T. F.; Abild-Pedersen, F.; Voss, J.; Luntz, A. C.; Nilsson, A. Ultrafast Adsorbate Excitation Probed with Subpicosecond-Resolution X-Ray Absorption Spectroscopy. *Phys Rev Lett* **2021**, *127* (1), 016802. https://doi.org/10.1103/PhysRevLett.127.016802.

(43) Tillborg, H.; Nilsson, A.; Martensson, N.; Andersen, J. N. Adsorption-Site-Dependent X-Ray-Absorption Spectroscopy - CO/H,H2/Ni(100). *Phys. Rev. B* **1993**, *47* (3), 1699–1702. https://doi.org/10.1103/PhysRevB.47.1699.

(44) Xin, H.; LaRue, J.; Öberg, H.; Beye, M.; Dell'Angela, M.; Turner, J.; Gladh, J.; Ng, M. L.; Sellberg, J. A.; Kaya, S.; Mercurio, G.; Hieke, F.; Nordlund, D.; Schlotter, W. F.; Dakovski, G. L.; Minitti, M. P.; Föhlisch, A.; Wolf, M.; Wurth, W.; Ogasawara, H.; Nørskov, J. K.; Öström, H.; Pettersson, L. G. M.; Nilsson, A.; Abild-Pedersen, F. Strong Influence of Coadsorbate Interaction on CO Desorption Dynamics on Ru(0001) Probed by Ultrafast X-Ray Spectroscopy and Ab Initio Simulations. *Phys. Rev. Lett.* **2015**, *114* (15), 156101. https://doi.org/10.1103/PhysRevLett.114.156101.

(45) Wang, H.-Y.; Schreck, S.; Weston, M.; Liu, C.; Ogasawara, H.; LaRue, J.; Perakis, F.; Dell'Angela, M.; Capotondi, F.; Giannessi, L.; Pedersoli, E.; Naumenko, D.; Nikolov, I.; Raimondi, L.; Spezzani, C.; Beye, M.; Cavalca, F.; Liu, B.; Gladh, J.; Koroidov, S.; Miedema, P. S.; Costantini, R.; Pettersson, L. G. M.; Nilsson, A. Time-Resolved Observation of Transient Precursor State of CO on Ru(0001) Using Carbon K-Edge Spectroscopy. *Phys Chem Chem Phys* **2020**. https://doi.org/10.1039/C9CP03677F.

(46) Nilsson, A.; Pettersson, Lars. G. M.; Norskov, J. K. *Chemical Bonding at Surfaces and Interfaces*; Elsevier, 2008.

(47) Hoffmann, F. M. M.; Weisel, M. D. D.; Peden, C. H. F. H. F. In-Situ FT-IRAS Study of the CO Oxidation Reaction over Ru(001). *Surf. Sci. Lett.* **1991**, *253* (1–3), A443. https://doi.org/10.1016/0167-2584(91)90376-3.

(48) Pettersson, L. G. M.; Nilsson, A. A Molecular Perspective on the D-Band Model: Synergy Between Experiment and Theory. *Top. Catal.* **2014**, *57* (1–4), 2–13. https://doi.org/10.1007/s11244-013-0157-4.

(49) Föhlisch, A.; Nyberg, M.; Bennich, P.; Triguero, L.; Hasselstrom, J.; Karis, O.; Pettersson, L. G. M.; Nilsson, A. The Bonding of CO to Metal Surfaces. *J. Chem. Phys.* **2000**, *112* (4), 1946–1958.

(50) Tetenoire, A.; Juaristi, J. I.; Alducin, M. Insights into the Coadsorption and Reactivity of O and CO on Ru(0001) and Their Coverage Dependence. *J. Phys. Chem. C* **2021**, *125* (23), 12614–12627. https://doi.org/10.1021/acs.jpcc.1c01618.

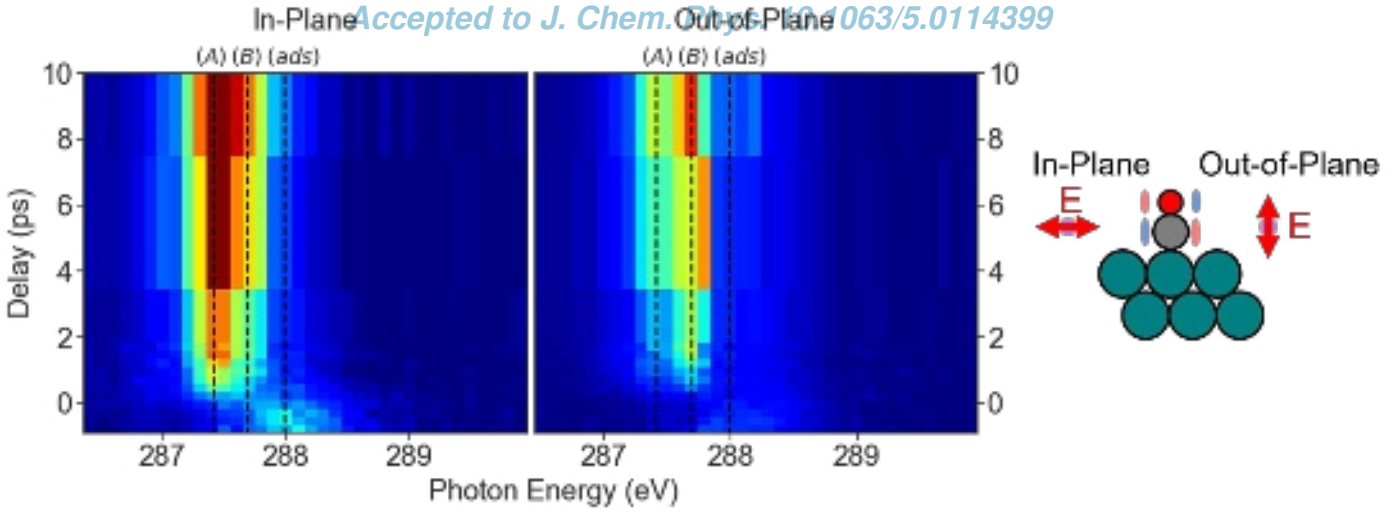

Accepted to J. Chem. Phys. 10.1063/5.0114399